Title

Spatial transcriptomics: Technologies, applications and experimental considerations

Journal

Genomics, 115(5)

ISSN

0888-7543

Authors

Wang, Ye

Liu, Bin

Zhao, Gexin

et al.

Publication Date

2023-09-01

DOI

10.1016/j.ygeno.2023.110671

Peer reviewed

HHS Public Access

Author manuscript

Genomics. Author manuscript; available in PMC 2023 October 13.

Published in final edited form as:

Genomics. 2023 September ; 115(5): 110671. doi:10.1016/j.ygeno.2023.110671.

Spatial transcriptomics: Technologies, applications and experimental considerations

Ye Wang[a,*,1], **Bin Liu**[b,1], **Gexin Zhao**[c], **YooJin Lee**[c], **Anton Buzdin**[d,e,f], **Xiaofeng Mu**[a], **Joseph Zhao**[c], **Hong Chen**[g], **Xinmin Li**[c,*]

[a] Clinical Laboratory, The Affiliated Qingdao Central Hospital of Medical College of Qingdao University, Qingdao 266042, China

[b] Departments of Medical Oncology, Cancer Hospital of China Medical University, Liaoning Cancer Hospital and Institute, Shenyang 110042, China

[c] UCLA Technology Center for Genomics & Bioinformatics, Department of Pathology & Laboratory Medicine, 650 Charles E Young Dr., Los Angeles, CA 90095, USA

[d] Shemyakin-Ovchinnikov Institute of Bioorganic Chemistry, Russian Academy of Sciences, Moscow 117997, Russia

[e] Moscow Institute of Physics and Technology, Moscow Region, 141701, Russia

[f] World-Class Research Center “Digital biodesign and personalized healthcare”, Sechenov First Moscow State Medical University, Moscow 119991, Russia

[g] Heilongjiang Academy of Traditional Chinese Medicine, No. 142, Sanfu Street, Xiangfang District, Harbin City, Heilongjiang Province 150036, China

Abstract

The diverse cell types of an organ have a highly structured organization to enable their efficient and correct function. To fully appreciate gene functions in a given cell type, one needs to understand how much, when and where the gene is expressed. Classic bulk RNA sequencing and popular single cell sequencing destroy cell structural organization and fail to provide spatial information. However, the spatial location of gene expression or of the cell in a complex tissue provides key clues to comprehend how the neighboring genes or cells cross talk, transduce signals and work together as a team to complete the job. The functional requirement for the spatial content has been a driving force for rapid development of the spatial transcriptomics technologies in the past few years. Here, we present an overview of current spatial technologies with a special focus

* Corresponding authors. yewang@qdu.edu.cn (Y. Wang), xinminli@mednet.ucla.edu (X. Li).

[1] Contributed equally: Ye Wang and Bin Liu.

Author contributions

YW, BL, HC and XL designed and wrote the manuscript. GZ and YL prepared figures and table, AB, XM and JZ wrote the part of manuscript and edited the entire manuscript. All authors reviewed and approved the submitted version.

Table 1 summarizes 5 key parameters of 8 discussed technologies to assist in choosing a suitable platform. As a general guideline, sequencing-based technologies are preferably used for an unbiased analysis for hypothesis generation, and imaging-based technologies are more suitable for a focused in-depth analysis for hypothesis testing.

Declaration of Competing Interest

The authors declare that they have no competing interests.

on the commercially available or currently being commercialized technologies, highlight their applications by category and discuss experimental considerations for a first spatial experiment.

Keywords

Spatial transcriptomics; RNA sequencing; 10× Visium; GeoMx DSP; CosMx SMI; MERFISH; Stereo-seq; Xienum; BMKMANU S1000

1. Spatial transcriptomics technologies

The revolution in imaging, barcoding and sequencing technologies in combination with the painful loss of spatial information in popular single cell sequencing have together driven rapid development of spatial transcriptomics (ST) technologies in the past 5 years. Seven ST technologies have been commercially released and at least one more is in the process of commercialization. ST technologies broadly fall into two categories: imaging-based and sequencing-based technologies [1,2]. The key difference between imaging-based and sequencing-based spatial transcriptomics technologies lies in their distinct approaches to determine the spatial localization and abundance of specific mRNA molecules within a tissue. Imaging-based technologies utilize fluorescent signatures and their intensity to decode the targeted gene and its abundance, while sequencing-based technologies rely on spatial barcodes on an array to restore the spatial position of the targeted gene in the tissue and use next-generation sequencing to determine its expression level. Below, we will discuss the core technologies, key parameters, advantages and disadvantages of eight spatial technologies that are commercially available now or will be available in 2023.

1.1. Imaging-based technologies

Contemporary imaging-based ST technologies are based on highly multiplexed single molecule fluorescence in situ hybridization (smFISH), and integrate histology, molecular and imaging tools into one box without requiring sequencing. The overall workflow and principles are very much similar across the various platforms. The workflow includes slide preparation, tissue permeabilization, fluorescent probe hybridization, imaging, color decoding and spatial mapping. The differences between available platforms are in probe design, hybridization and color decoding. As of December 2022, there are four commercially available imaging-based platforms: Molecular Cartography, MERSCOPE, 10× Xenium and CosMx Spatial Molecular Imager.

Molecular Cartography (MC) from Resolve Biosciences was commercially launched in the last quarter of 2021. This technology adopted the sequential FISH (seqFISH) approach using a three-probe hybridization strategy. Briefly, more than twenty gene-specific primary probes first hybridize to a targeted transcript at different positions (use of more probes for the same gene boosts signal-to-noise ratio for high detection sensitivity). Secondary probes linked with a specific barcoding system hybridize to hangout tail regions of the primary probe, followed by third hybridizations to the barcode regions on the secondary probes with fluorescent probes (Fig. 1A). After imaging, the secondary and tertiary probes are removed, followed by a second round of secondary and tertiary probe hybridizations

with a different set of fluorophores. A total of eight consecutive rounds of fluorescent hybridization, imaging, color stripping and rehybridization create a fluorescent signature with a different combination of fluorophores, which is specific to the targeted gene [3,4].

The MC technology has high sensitivity and specificity, which is suitable for detection of rare transcripts in the cells. However, MC technology labels the probes in every round, and optical crowding limits the number of detected transcripts. The current product detects a panel of 100 genes with the potential for future expansion.

MERSCOPE from Vizgen was the first commercially launched platform in August 2021 (MERFISH-based technology). MERFISH technology has 3 key components: combinatory labeling, error-robust barcoding and sequential imaging. In brief, each gene is pre-assigned a binary barcode, a series of “0 s” and “1 s”. Thirty to fifty gene-specifc probes physically imprinting the binary barcode hybridize to different positions on a targeted gene. Each probe has a target region that binds to transcripts of interest and has hangout tails for readout binding. The fluorescently labeled or unlabeled secondary probes hybridize to the tails of the first probe to read out the barcode through multiple rounds of imaging (Fig. 1B). In any round of hybridization, detecting fluorescence will decode as “1” and no fluorescence as “0”. After imaging, the fluorescent signal is stripped, and new readout probes are introduced in subsequent rounds to readout the remainder of the barcode. As opposed to MC technology where the probes are fluorescently labeled in each round of hybridization, only a subset of probes are fluorescently labeled in each round of imaging in the MERFISH technology. Specifically, a MERFISH barcode usually has four “1 s” in a given order, i.e., the fluorescent signal for a barcode will only be detected four times for an assigned gene throughout imaging rounds. The optical barcode generated through multiple rounds of imaging will then be used to match with the pre-assigned barcode and resolve the identity and quantity of different RNA species. This binary labeling strategy effectively mitigates the optical crowding issue and helps detect and correct errors during the hybridization [5].

Xenium from 10× Genomics launched in December 2022, representing the third commercially available imaging-based spatial platform. Xenium was modified and further developed based on the CARTANA technology that was acquired by 10× Genomics in 2020. Xenium is a hybrid of in situ sequencing (ISS) and in situ hybridization (ISH) technologies. Firstly, an average of 8 padlock probes [6] with gene-specifc barcodes hybridize to a target transcript. After highly specific probe ligation, circular DNA probes are enzymatically amplified. Secondly, an oligo probe labeled with a pre-assigned fluorophore hybridizes to a gene-specifc barcode built into the padlock probe. After the fluorescent color is imaged and removed, successive rounds of the same process with a different fluorophore are repeated on average 8 times to generate an optical signature for target gene identification (Fig. 1C) [7].

The padlock probe offers two advantages: the gene-specifc ligation minimizes mispriming and increase hybridization specificity, and the padlock probe amplification makes multiple copies of the barcode, enabling a bright and high signal to noise ratio for imaging.

The CosMx Spatial Molecular Imager (CosMx SMI) from Nanostring started shipping in December 2022. The hybridization strategy of CosMx is similar to that of MERSCOPE in

principle. After the tissue is permeabilized, a pool of 5 gene-specific probes is hybridized to different positions on the targeted gene. Each probe has a 30–50 nucleotide target binding domain and around 100 nucleotide readout domain. Each set of 5 gene-specific probes has its unique sequence in the target-binding domain, whereas all 5 gene-specific probes from each set share the same sequence in the readout domain. This design enables the highest sensitivity detection in FFPE tissue, in which RNA is often fragmented. The readout domain includes 16 sub-domains. After the probes are hybridized, the slide is assembled and inserted into CosMx SMI. The fluorescently labeled secondary probes are introduced and hybridized to one of the subdomains of the primary probe. The secondary probe also contains a primary probe binding domain linked with a fluorescently labeled domain through a UV cleavable linker. The fluorescently labeled domain contains multiple fluorophore dyes to boost signal intensity (Fig. 1D). After the image is taken, UV cleaves the labeling domain.

This process is repeated 16 times. The combination of fluorophores dictated by the secondary probes annealing to the hybridization subdomain on the primary probe, generated from 16 rounds of hybridization, is specific to the targeted gene. The combination of 4 fluorescent colors and 16 sub-domains allows CosMx SMI to profile more genes than other 3 imaging-based platforms. Currently, CosMx SMI supports simultaneous imaging and quantification of 1000+ RNA and 64+ protein targets at subcellular resolution [8].

The imaging-based spatial technologies can provide single cell or subcellular resolution with high RNA capturing efficiency. However, due to some common technical limitations, such as optical crowding, increased risk of binding error with increasing number of hybridization rounds, long imaging time and small imaging area, current commercial platforms can only profile a few hundred to a thousand genes. In the next section, we will discuss sequencing-based spatial technologies that overcome the above technical limitations.

1.2. Sequencing-based technologies

Most sequencing-based technologies combine classic microarray technologies with current next generation sequencing technologies to make spatial localization of gene expression possible. Briefly, the microarray attaches thousands to millions of oligoes that include spatial barcode sequences, poly (dT) and other domains. After the tissue section placed on the array is imaged and permeabilized, RNA is released from the tissue and hybridized to poly (dT) on the array. The cDNA and library are made on and off the array, respectively. Based on the spatial barcode sequence in the library which is copied from the array during reverse transcription, transcripts can be mapped back to the original location on the tissue after sequencing. Three sequencing-based platforms are commercially available now: 10× Visium, GeoMx Digital Spatial Profiler (DSP) and BMKMANU S1000. Stereo-seq is expected to become commercially available in 2023. 10× Visium, BMKMANU S1000 and Stereo-seq use array technology with similar overall workflow while GeoMx DSP adopts a different barcode technology. For the convenience of discussion, we will discuss the three microarray-based technologies first.

Visium from 10× Genomics was developed based on the Spatial Transcriptomics technology that 10× Genomics acquired in 2018 [9]. The microarray chip coated with spatially barcoded

RNA-binding oligonucleotides represents the core technology of Visium. The spatial barcode built into the oligonucleotides, acting as a messenger, is transferred to the cDNA during library construction, allowing localization of the transcripts back to the original tissue after sequencing (Fig. 2A). The Visium technology can work with fresh tissues, as well as Formalin-Fixed Paraffin-Embedded (FFPE) tissues with a slightly modified RNA capturing strategy [10].

In the fresh frozen workflow, the mRNA released from the tissue section directly binds to the poly(dT) region of adjacent capture probes on the array, while the FFPE workflow adopts a probe hybridization strategy to address the poor RNA quality from FFPE tissues. In the FFPE workflow, the tissue section on the array is treated to remove cross-linking and be permeabilized. A pair of adjacent probes in the protein-coding region is hybridized to the targeted gene. After ligation, the gap between the probe pair is sealed to form one longer probe. The poly-A tail linked to one of the probes on the 3'end is then captured by the poly (dT) on the array. The double stranded cDNA is synthesized by probe extension, and a sequencing library is made via sample index PCR.

The Visium platform does not require any special instruments, and can be easily adopted by a molecular lab equipped with traditional tissue section tools. The technical challenge of the Visium technology is the requirement to precisely transfer a tissue section to the 6.5 mm × 6.5 mm capturing areas of the Visium array. In addition, direct transfer of the tissue section to the array is often suboptimal without the investigator's evaluation. To address these two issues, 10× Genomics has released a Visium CytAssist instrument, which was designed to simplify the Visium workflow by facilitating the transfer of the tissue section from a standard glass slide to the Visium array. With CytAssist, investigators can use either pre-sectioned tissue on glass slides or FFPE blocks. This option maximizes the sample selection for Visium experiments and also allows evaluation of the quality of tissue sections using standard histological techniques before transferring to the Visium slide.

BMKMANU S1000 from Biomarker is technologically similar to 10× Visium with two key differences. Instead of directly attaching oligos to a capturing area with around 5000 barcoded spots as in the 10× Visium (where the position of each oligo on the array is known), S1000 attaches the oligo probes (Read 1 + Spatial Barcode+Unique Molecular Identifer+Poly (dT)) to beads that are embedded in the 2.2 million microwells on a 6.8 mm × 6.8 mm capturing area. The position of each oligo in the microwell is determined by several rounds of fluorescent hybridizations. Secondly, the diameter of S1000 microwells is 2.5 μm and center to center distance is 4.8 μm, while the 10× Visium has a 50um diameter spot size and a 100um center to center distance (Fig. 2B). This size difference leads to different spatial resolutions between two platforms.

The S1000 has a flexible experimental design with from 1 to 8 capturing areas per slide. Users can perform whole transcriptome analysis at 100um resolution or compromise the number of genes detected at a single cell resolution (5 μm). The noticeable weakness of S1000 is its inability to analyze an FFPE sample.

Stereo-seq from MGI uses the DNA nanoball (DNB) technology for in situ RNA capture and RNA localization (Fig. 2C). Similar to 10× Visium and S1000, synthesized oligos contain several domains including random barcoded sequences, the coordinate identity (CID), molecular identifiers (MID) and poly (dT) sequence. Instead of directly attaching the oligos to the array in the 10× Visium or attaching the oligos on the beads in the S1000, Stereo-seq oligos are circularized, and used as a template to generate DNB by rolling circle amplification. The DNBs are docked in a grid-patterned array of spots to make the Stereo-seq capture chips [11]. The spatial position of each DNB is determined by sequencing the 25-nt CID. The size of DNB is approximately 0.2um in diameter with a center-to-center distance of 0.5um, which is significantly smaller than the S1000, providing sub-cellular resolution.

The Stereo-seq technology is particularly suitable for developmental biology with its large array, but is currently not available for FFPE samples. MGI offers several different sizes of Stereo-seq arrays from 1 cm × 1 cm to 13.2 cm × 13.2 cm. Stereo-seq libraries can only be sequenced on MGI sequencers such as T7, which will limit their wide adoption after commercialization.

GeoMx Digital Spatial Profiler (DSP) from Nanostring Technologies uses a completely different strategy to make libraries and obtain spatial information. It first designs a pool of ~20,000 gene-specifc probes genome wide, and links each of the probes to a unique, probe specific DSP barcode through a UV cleavable linker. The probe pool is hybridized to mRNA targets on a tissue slide overnight and washed the next morning. The slide is then stained using fluorescently labeled antibodies (markers) for the cell types of interest, and imaged using the GeoMx DSP instrument. Based on the staining result, multiple regions of interest (ROIs) are selected. UV light is then applied to release and collect the DSP barcodes from selected ROIs, followed by library construction and sequencing [12,13]. The counts of a gene-specifc DSP barcode represent the abundance of the corresponding mRNA, and the gene-specifc DSP barcodes are mapped back to the tissue section of the spatially defined ROIs (Fig. 2D). This spatially defined ROI enables investigators to understand the gene expression patterns or molecular interactions within that specific spatial context.

GeoMx DSP can place more samples on the same slide without being limited by predesigned capturing areas like array-based platforms. It only makes libraries from the selected ROIs, and thus is more cost effective per sample compared to other sequencing-based platforms. In addition, users have an option to add some custom probes to the probe pool to ensure genes of interest are detected. The practical challenges of GeoMx DSP are its cell marker selection and fluorescent staining. The antibody markers sometimes produce unsatisfactory staining and need to be validated before the real experiment.

Sequencing-based ST technologies can provide whole transcriptome analysis with a large imaging area and short scanning time, but they have relatively lower RNA capturing efficiency and cannot provide single cell resolution for two commonly used platforms: 10× Visium and GeoMx DSP. It is worth noting that an upcoming Stereo-seq platform next year combines the strengths of sequencing-and imaging-based technologies, and provides whole transcriptome analysis at single cell resolution.

2. Applications for basic, translational and clinical research

ST has broad applications in developmental biology, immunology, oncology and neuroscience in disease and health tissues for human, mouse and other species. It can answer many biological questions that are applicable to single cell sequencing technology and many other important questions that single cell technology is unable to answer. Of importance, ST technologies have great potential in clinical applications with need for higher sensitivity and accuracy, including early diagnosis, prognosis, spatial marker identification, drug development, clinical trials and so on. In this section, we will highlight recent applications in representative areas.

2.1. Spatiotemporal analyses of tissue development

ST technologies have been widely used in embryo, tissue, and organ development in various species, documented by a large body of literature [2,14–16]. It is of particular note for studying embryogenesis [17,18]. How a zygote develops into a highly complex organism in a precisely regulated manner is one of the most important scientific questions. Several methodologies have been applied to study mammalian embryogenesis. However, lack of cellular structural organization information, lack of contextual microenvironments, low spatial resolution, a small number of genes, or a combination of these factors have limited the power of those approaches. ST technology is an ideal tool to systematically and coherently answer this fundamental and long-standing question. It allows investigation of spatiotemporal transcriptomic dynamics in the natural cell ecosystem in relation to cell fate specification, cell-cell interaction, and organ formation, i.e., we are able to visualize an entire “motion picture” of embryonic development from different dimensions in situ.

Taking advantage of the large field of view of Stereo-seq technology, Chen et al. studied spatiotemporal transcriptomics of mouse organogenesis using 53 sagittal sections from entire mouse embryos spanning E9.5–E16.5 [19]. The study identified tissue- or site-specific gene expression profiles, and visualized dynamic changes of these profiles over different developmental stages. The high resolution, directional transcriptomic changes in a time course provide functional insights regarding cell fate differentiation, cell migration, regional specification and organ formation. Using spatial consistency-based clustering (SCC) methods and unsupervised clustering of the gene-by-cell matrix and uniform manifold approximation and projection (UMAP) visualization, Chen et al. established spatial relationships between distinct gene signatures and heterogenous cell types, cell type locations and specific anatomic regions. The data set was subsequently used to generate a mouse organogenesis spatiotemporal transcriptomic atlas (MOSTA). This comprehensive resource is a foundation for future studies of organogenesis in mouse or other species.

2.2. Spatial atlases of specific tissues or regions

ST technologies can provide an unbiased spatial map of a tissue and have generated several expandable reference tissue atlases, including human kidney tissue atlases in health and disease [20], spatial multiomic maps of cardiac remodeling [21], the human lung [22], and several brain tissue atlases from hypothalamic pre-optic regions [23], hippocampus [24] and cerebellum [25]. The technology also significantly empowers a few influential atlas

initiatives, including Human Lung Cell Atlas 1.0 (Chan Zuckerberg initiative), NIH Brain Initiative Cell Atlas, and Human Cell Atlas Initiative.

Ortiz et al. generated an ST atlas of entire brain regions that include 15,326 unique genes [26]. In this study, authors mapped known subdivisions and the borders of the entire nervous system, identified new area- and layer-specific subregions in the isocortex and hippocampus, as well as new subdivisions of striatum using unsupervised classification. This study demonstrated that ST data alone are able to dissect and map the complex spatial neuroanatomical organization of the brain with well-defined regional boundaries. It has laid a foundation for investigating the structure-function relationship of specific brain regions for other species. By cross-species comparison, it will provide critical information for a comprehensive understanding of the diversity of neuron types and their circuits in humans.

2.3. Molecular mechanisms of gene or cellular dysregulation in disease

The current understanding of the molecular mechanisms underlying various diseases is limited by an inability to directly examine disease-causing cells and their microenvironment under natural conditions. ST technology has opened new opportunities in this dimension. The use of ST identified ZBTB11 as a regulator of cardiomyocyte degeneration in arrhythmogenic cardiomyopathy [27] and an unknown population of neurons that regulate fever response and other sickness symptoms [27,28]. It has also been used to provide molecular insights into the coronavirus disease 2019 [29,30], infectious and inflammatory processes [31–33], and disease associated signaling and pathways in amyotrophic lateral sclerosis [34], as well as the dorsolateral prefrontal cortex of schizophrenia patients [10,35] and Alzheimer’s disease.

Of particular interest, Niño et al. used 10× Visium technology to uncover spatially resolved cellular and molecular host-microbe interactions in oral squamous cell carcinoma and colorectal cancer [36]. Tumor-associated bacteria have an active role in cancer development, but the identity and host cell types of these bacteria have not yet been understood. Using 10× Visium and GeoMx DSP technologies, the authors demonstrated that bacteria are associated with malignant cells with lower levels of Ki-67 compared to the tumor regions absent of bacteria, and those bacteria are highly immunosuppressive in the tumors. The interaction between host cells and bacteria altered the transcriptional pathways that are involved in inflammation, metastasis, cell dormancy and DNA repair. The data demonstrated that the distribution of microbiota in the tumors is not a random event, but are functionally organized to promote cancer progression.

2.4. Cellular heterogeneity and microenvironment in tumors

The continuous contest between extrinsic immune cells and intrinsic tumor cells shapes tumor progression and metastasis. Quantitative analysis of tumor heterogeneity and spatiotemporal characterization of tumor immune microenvironments can provide essential information for understanding tumor metastasis and developing novel therapies. ST technologies allow comprehensive analysis of the transcriptomic signatures of tumors and their associated cells, and reveal spatial tumor heterogeneity and its entire microenvironment [37–40].

A relatively early study (in terms of ST technology) used ST profiles from around 6750 tissue regions across different tissue components to construct a detailed spatial map for intra-tumor heterogeneity in prostate cancer [41]. The map showed remarkably heterogeneous transcriptomic profiles at each tissue region and exhibited a gradient gene expression profile in healthy cells adjacent to tumor cells, a warning for using normal tissue adjacent to tumor as a normal control in experiment design. A recent study explored the immune landscape of liver metastasis of colorectal cancer [42]. In this study, the authors investigated ST dynamics of the immune microenvironment of 97 samples from 24 matched (primary and metastasized) liver patients. The study revealed extraordinary immune microenvironment reprogramming during metastasis, such as immunosuppressive MRC1 + CCL18+ M2-like macrophages. Single cell Metabolism analysis [40] showed that those macrophages have enhanced metabolic activity and can be reversed by effective neoadjuvant chemotherapy in responsive patients. Interestingly, the same treatment triggered more immunosuppressive environments in nonresponse patients. This observation suggests that the metabolism pathway could be a potential drug target in metastasized patients.

2.5. Cell types and states

ST techniques have further enhanced the power of single cell sequencing technologies in identifying and characterizing cell types and states. The functional elucidation of different cell types requires their physical localization and connectivity. The spatial dimension of ST technologies enables the functional analysis of cell populations, neighbor cell interactions and cellular structural organization. Numerous publications have documented the progress made in this aspect in the past few year s [23,43–46].

Fang et al. applied the MERFISH technology to analyze the spatial distributions of cell types within the human and mouse cortexes, and identified >100 transcriptionally distinct cell populations in the human middle and superior temporal gyrus [47]. The analysis found that the association patterns of specific cell types are different between the mouse and human brains. Humans have more specific neurons and increased interactions between neurons and non-neuronal cells compared to mice. In a spinal cord injury study [48], the ST technology discovered a single population of excitatory interneurons nested within the intermediate laminae. This unique cell population is essential for the recovery of walking with epidural electrical stimulation following spinal cord injury.

Using the EcoTyper tool, Luca et al. identified 69 transcriptionally defined cell states across 12 major cell lineages of 16 types of human carcinoma [49]. Most of the cell states are ubiquitous across tumor types, indicating fundamental patterns of cellular organization in human carcinoma. Further analysis of cell-state co-occurrence patterns identified ten clinically distinct, evolutionarily conserved multicellular communities, some of which are associated with adverse survival and others associated with early cancer development.

2.6. Spatially resolved biomarkers for diseases and treatments

ST technologies have greatly facilitated the development of more accurate and sensitive molecular, cellular and microstructural biomarkers spatially, leading to improved diagnosis, prognosis and disease treatment. Some examples include a 6-gene signature for the

prediction of patient survival in hepatocellular carcinoma [50], the GATA3 mutation for relapse in breast cancer [51], CD56+ immune cells for the prediction of outcomes of a PD-1 checkpoint blockade in NSCLC [52], CDH12-enriched epithelial subpopulation for the prediction of poor outcomes following surgery, superior responses to immune checkpoint therapy in the bladder [53], Trem2hi- enriched macrophages in late-stage infarcted heart leading to significant functional and structural improvements in infarcted hearts [54], and leucine zipper transcription factor like 1 as a candidate effector gene at a COVID-19 risk locus [55].

Spatial microstructural biomarkers, identified by using ST technology, are particularly interesting. In 2020, Petitprez et al. first reported that the presence of intratumoral tertiary lymphoid structures (TLSs) is associated with improved outcomes in advanced soft-tissue sarcoma (STSs) patients, and suggested that TLS presence in advanced STS is a potential predictive biomarker for patients' selection for pembrolizumab treatment [56]. Later, a multicohort phase 2 study of pembrolizumab (PEMBROSARC) showed that the 6-month non-progression rate and objective response rate in patients selected based on the presence of TLSs are significantly better than those in all-comer patients. This clinical trial confirmed that TLS is an efficient microstructure biomarker for STS patient selection for immunotherapy [57].

3. Considerations for a first ST experiment

In this article, we reviewed 8 different platforms that use different strategies to resolve spatial information and capture transcriptome profiles. These technologies have different technical capabilities and limitations. One specific technology may be suitable only for certain species, tissue types or experimental aims. Users should carefully consider these limitations and capabilities at the experimental design stage to ensure the chosen platform is suitable for your tissue type and experimental aim. In the following section, we provide a summary of essential considerations for choosing a suitable spatial technology.

3.1. Biological question

In the experimental planning stage, you should clearly define your biological questions to ensure that spatial technology is appropriate, i.e., spatial content in the data set is essential to answer your questions, and cannot be satisfactorily addressed by other simpler or more cost effective technologies, such as bulk RNAseq.

3.2. Species and tissue type

What species and tissue type are available for your study? Some technologies are limited to certain species. For example, GeoMx DSP can only work with human and mouse tissues while 10× Visium suits many species. Both technologies are amenable to fresh frozen tissues as well as FFPE tissue, but Molecular Cartography and BMKMANU S1000 are only applicable to fresh frozen tissue. In the case of 10× Visium, optimization is needed to determine the best permeabilization time for untried tissue types.

3.3. RNA integrity

Is your RNA integrity sufficient for the chosen technology? If you use FFPE tissue, RNA quality can be a potential problem and needs to be verified before the experiment. 10× Visium and GeoMx DSP FFPE protocols recommend —the percentage of RNA fragments above 200 nucleotides ≥ 50%, although less ideal RNA integrity may also produce usable data when the sample is irreplaceable, such as for clinical specimen.

3.4. Tissue size

Do you need a large area to capture the necessary information? Different technologies have different defined capturing or imageable areas. 10× Visium has a capturing area of 6.5 mm × 6.5 mm, MERSCOPE has an imageable area of 10 mm × 10 mm, while Stereo-seq technology has a slide with a capturing area as large as 13.2 cm × 13.2 cm. GeoMx DSP requires 3 replicates of ROIs for statistical analysis with their software, and the tissue section should be large enough for 3 ROI selections when considering GeoMx DSP.

3.5. The number of genes profiled

Do you need whole transcriptome analysis or a focused gene panel? In general, imaging-based technologies can only profile a limited number of genes due to optical crowding and other issues, ranging from 100 genes for Molecular Cartography to 1000 genes for CoxMx SMI. The sequencing-based platforms allow whole transcriptome analysis. In our hands, 10× Visium can recover ~16,762 genes/capturing area, and GeoMx DSP can detect ~11,328 genes/ROI on average.

3.6. Spatial resolution

The most commonly used spatial platforms today, such as 10× Visium and GeoMx DSP, cannot provide single cell resolution. The resolution of 10× Visium is limited by its 50um spot size (a typical eukaryotic cell size is around 10um). GeoMx DSP can technically select ROIs as small as a single cell, but signal to noise ratio from such a small ROI is practically too low to analyze the data meaningfully. If the experimental design requires single cell resolution, imaging-based technologies should be considered.

3.7. RNA capturing efficiency

Different platforms have highly variable RNA capturing efficiency, ranging from ~95% to as low as ~30%. Generally, imaging-based technologies have a significantly higher capturing efficiency than sequencing-based ones. If you are interested in low expressors, such as transcription factors, you should consider imaging-based platforms.

3.8. Analyzed analyte

Spatial proteogenomics represents an exciting future direction in the field of spatial genomics. If you have a precious clinical sample and want to analyze RNA and protein simultaneously on the same slide, GeoMx DSP is the only platform for consideration. Nanostring recently released a GeoMx DSP spatial proteogenomic protocol that enables both protein and RNA expression analysis from a single FFPE slide.

3.9. The number of samples

Finally, sample number should also be taken into consideration at the experimental design stage. Imaging-based platforms take 2–7 days to scan a slide compared to ~30 min with sequencing-based platforms. If you propose processing a large number of samples, imaging-based platforms may not be practical.

4. Concluding remark

Here, we have explored eight spatial transcriptomics technologies that are currently available or will be introduced in 2023. These advanced technologies exhibit distinct strengths and weaknesses, which are reflected in five key parameters (Table 1). The selection of a particular technology requires careful consideration of these parameters and alignment with the experimental objectives. In general, sequencing-based technologies are well-suited for hypothesis generation and research development, while imaging-based technologies are more appropriate for hypothesis testing and potential clinical applications in the future.

Several technological limitations remain to be addressed in the field. These include limited multiplexing and throughput of imaging based technologies, as well as the low spatial resolution and RNA capturing efficiency of sequencing-based technologies. The future endeavors will necessitate additional advancements in spatial multiomics methods and the integration of multi-dimensional datasets. These datasets should encompass the interpretation of spatial DNA alteration, transcriptional regulation, epigenetic modification, and metabolic reprogramming. The incorporation of AI-guided high dimensional cellular phenotyping data, using, for example, recently launched Deepcell technology [58], represents another future trajectory. The development of new computational and creative analytical tools to effectively analyze the resulting data will be a crucial next task.

Funding

This work was supported by NIH grans 2P30CA016042–45, 1R01CA241927–01A1, and the National Natural Science Foundation of China (No. 81670822), Qingdao Key Research Project (No. 17–3-3–10-nsh and 19–6-1–3-nsh) and Qingdao Key Health Discipline Development Fund. AB contribution was supported by the Ministry of Science and Higher Education of the Russian Federation within the framework of state support for the creation and development of World-Class Research Centers “Digital biodesign and personalized healthcare” No 075–15-2022–304.

Data availability

The authors do not have permission to share data.

References

[1]. Moffitt JR, Lundberg E, Heyn H, The emerging landscape of spatial profiling technologies, Nat. Rev. Genet. 23 (2022) 741–759. [PubMed: 35859028]

[2]. Rao A, Barkley D, Franca GS, Yanai I, Exploring tissue architecture using spatial transcriptomics, Nature 596 (2021) 211–220. [PubMed: 34381231]

[3]. Groiss S, Pabst D, Faber C, Meier A, Bogdoll A, Unger C, Nilges B, Strauss S, Föderl-Höbenreich E, Hardt M, Geipel A, Reinecke F, Korfhage C, Zatloukal K, Highly resolved spatial transcriptomics for detection of rare events in cells, bioRxiv (2021), 2021.2010.2011.463936.

[4]. D'Gama PP, Qiu T, Cosacak MI, Rayamajhi D, Konac A, Hansen JN, Ringers C, Acuna-Hinrichsen F, Hui SP, Olstad EW, Chong YL, Lim CKA, Gupta A, Ng CP, Nilges BS, Kashikar ND, Wachten D, Liebl D, Kikuchi K, Kizil C, Yaksi E, Roy S, Jurisch-Yaksi N, Diversity and function of motile ciliated cell types within ependymal lineages of the zebrafish brain, Cell Rep. 37 (2021), 109775. [PubMed: 34610312]

[5]. Chen KH, Boettiger AN, Moffitt JR, Wang S, Zhuang X, RNA imaging. Spatially resolved, highly multiplexed RNA profiling in single cells, Science 348 (2015) aaa6090. [PubMed: 25858977]

[6]. Nilsson M, Krejci K, Koch J, Kwiatkowski M, Gustavsson P, Landegren U, Padlock probes reveal single-nucleotide differences, parent of origin and in situ distribution of centromeric sequences in human chromosomes 13 and 21, Nat. Genet. 16 (1997) 252–255. [PubMed: 9207789]

[7]. Janesick A, Shelansky R, Gottscho AD, Wagner F, Rouault M, Beliakoff G, de Oliveira MF, Kohlway A, Abousoud J, Morrison CA, Drennon TY, Mohabbat SH, Williams SR, Taylor SEB, High resolution mapping of the breast cancer tumor microenvironment using integrated single cell, spatial and in situ analysis of FFPE tissue, bioRxiv (2022), 2022.2010.2006.510405.

[8]. He S, Bhatt R, Brown C, Brown EA, Buhr DL, Chantranuvatana K, Danaher P, Dunaway D, Garrison RG, Geiss G, Gregory MT, Hoang ML, Khafizov R, Killingbeck EE, Kim D, Kim TK, Kim Y, Klock A, Korukonda M, Kutchma A, Lewis ZR, Liang Y, Nelson JS, Ong GT, Perillo EP, Phan JC, Phan-Everson T, Piazza E, Rane T, Reitz Z, Rhodes M, Rosenbloom A, Ross D, Sato H, Wardhani AW, Williams-Wietzikoski CA, Wu L, Beechem JM, High-plex imaging of RNA and proteins at subcellular resolution in fixed tissue by spatial molecular imaging, Nat. Biotechnol. (2022).

[9]. Stahl PL, Salmen F, Vickovic S, Lundmark A, Navarro JF, Magnusson J, Giacomello S, Asp M, Westholm JO, Huss M, Mollbrink A, Linnarsson S, Codeluppi S, Borg A, Ponten F, Costea PI, Sahlen P, Mulder J, Bergmann O, Lundeberg J, Frisen J, Visualization and analysis of gene expression in tissue sections by spatial transcriptomics, Science 353 (2016) 78–82. [PubMed: 27365449]

[10]. Maynard KR, Collado-Torres L, Weber LM, Uytingco C, Barry BK, Williams SR, Catallini JL 2nd, Tran MN, Besich Z, Tippani M, Chew J, Yin Y, Kleinman JE, Hyde TM, Rao N, Hicks SC, Martinowich K, Jaffe AE, Transcriptome-scale spatial gene expression in the human dorsolateral prefrontal cortex, Nat. Neurosci. 24 (2021) 425–436. [PubMed: 33558695]

[11]. Chen A, Liao S, Cheng M, Ma K, Wu L, Lai Y, Yang J, Li W, Xu J, Hao S, Chen X, Liu X, Huang X, Lin F, Tang X, Li Z, Hong Y, Fu D, Jiang Y, Peng J, Liu S, Shen M, Liu C, Li Q, Wang Z, Wang Z, Huang X, Yuan Y, Volpe G, Ward C, Muñoz-Cánoves P, Thiery JP, Zhao F, Li M, Kuang H, Wang O, Lu H, Wang B, Ni M, Zhang W, Mu F, Yin Y, Yang H, Lisby M, Cornall RJ, Uhlen M, Esteban MA, Li Y, Liu L, Wang J, Xu X, Large field of view-spatially resolved transcriptomics at nanoscale resolution, bioRxiv (2021), 2021.2001.2017.427004.

[12]. Li X, Wang CY, From bulk, single-cell to spatial RNA sequencing, Int. J. Oral. Sci. 13 (2021) 36. [PubMed: 34782601]

[13]. Merritt CR, Ong GT, Church SE, Barker K, Danaher P, Geiss G, Hoang M, Jung J, Liang Y, McKay-Fleisch J, Nguyen K, Norgaard Z, Sorg K, Sprague I, Warren C, Warren S, Webster PJ, Zhou Z, Zollinger DR, Dunaway DL, Mills GB, Beechem JM, Multiplex digital spatial profiling of proteins and RNA in fixed tissue, Nat. Biotechnol. 38 (2020) 586–599. [PubMed: 32393914]

[14]. Zibetti C, Deciphering the retinal epigenome during development, disease and reprogramming: advancements, challenges and perspectives, Cells 11 (2022).

[15]. Garcia-Alonso L, Lorenzi V, Mazzeo CI, Alves-Lopes JP, Roberts K, Sancho-Serra C, Engelbert J, Mareckova M, Gruhn WH, Botting RA, Li T, Crespo B, van Dongen S, Kiselev VY, Prigmore E, Herbert M, Moffett A, Chedotal A, Bayraktar OA, Surani A, Haniffa M, Vento-Tormo R, Single-cell roadmap of human gonadal development, Nature 607 (2022) 540–547. [PubMed: 35794482]

[16]. Zhu Y, Sousa AMM, Gao T, Skarica M, Li M, Santpere G, Esteller-Cucala P, Juan D, Ferrandez-Peral L, Gulden FO, Yang M, Miller DJ, Marques-Bonet T, Imamura Kawasawa Y, Zhao H, Sestan N, Spatiotemporal transcriptomic divergence across human and macaque brain development, Science 362 (2018).

[17]. Wang M, Hu Q, Lv T, Wang Y, Lan Q, Xiang R, Tu Z, Wei Y, Han K, Shi C, Guo J, Liu C, Yang T, Du W, An Y, Cheng M, Xu J, Lu H, Li W, Zhang S, Chen A, Chen W, Li Y, Wang X, Xu X,

Hu Y, Liu L, High-resolution 3D spatiotemporal transcriptomic maps of developing Drosophila embryos and larvae, Dev. Cell 57 (2022), 1271–1283 e1274. [PubMed: 35512700]

[18]. Liu C, Li R, Li Y, Lin X, Zhao K, Liu Q, Wang S, Yang X, Shi X, Ma Y, Pei C, Wang H, Bao W, Hui J, Yang T, Xu Z, Lai T, Berberoglu MA, Sahu SK, Esteban MA, Ma K, Fan G, Li Y, Liu S, Chen A, Xu X, Dong Z, Liu L, Spatiotemporal mapping of gene expression landscapes and developmental trajectories during zebrafish embryogenesis, Dev. Cell 57 (2022), 1284–1298 e1285. [PubMed: 35512701]

[19]. Chen A, Liao S, Cheng M, Ma K, Wu L, Lai Y, Qiu X, Yang J, Xu J, Hao S, Wang X, Lu H, Chen X, Liu X, Huang X, Li Z, Hong Y, Jiang Y, Peng J, Liu S, Shen M, Liu C, Li Q, Yuan Y, Wei X, Zheng H, Feng W, Wang Z, Liu Y, Wang Z, Yang Y, Xiang H, Han L, Qin B, Guo P, Lai G, Munoz-Canoves P, Maxwell PH, Thiery JP, Wu QF, Zhao F, Chen B, Li M, Dai X, Wang S, Kuang H, Hui J, Wang L, Fei JF, Wang O, Wei X, Lu H, Wang B, Liu S, Gu Y, Ni M, Zhang W, Mu F, Yin Y, Yang H, Lisby M, Cornall RJ, Mulder J, Uhlen M, Esteban MA, Li Y, Liu L, Xu X, Wang J, Spatiotemporal transcriptomic atlas of mouse organogenesis using DNA nanoball-patterned arrays, Cell 185 (2022), 1777–1792 e1721. [PubMed: 35512705]

[20]. Hansen J, Sealfon R, Menon R, Eadon MT, Lake BB, Steck B, Anjani K, Parikh S, Sigdel TK, Zhang G, Velickovic D, Barwinska D, Alexandrov T, Dobi D, Rashmi P, Otto EA, Rivera M, Rose MP, Anderton CR, Shapiro JP, Pamreddy A, Winfree S, Xiong Y, He Y, de Boer IH, Hodgin JB, Barisoni L, Naik AS, Sharma K, Sarwal MM, Zhang K, Himmelfarb J, Rovin B, El-Achkar TM, Laszik Z, He JC, Dagher PC, Valerius MT, Jain S, Satlin LM, Troyanskaya OG, Kretzler M, Iyengar R, Azeloglu EU, P. Kidney Precision Medicine, A reference tissue atlas for the human kidney, Sci. Adv. 8 (2022) eabn4965. [PubMed: 35675394]

[21]. Kuppe C, Ramirez Flores RO, Li Z, Hayat S, Levinson RT, Liao X, Hannani MT, Tanevski J, Wunnemann F, Nagai JS, Halder M, Schumacher D, Menzel S, Schafer G, Hoeft K, Cheng M, Ziegler S, Zhang X, Peisker F, Kaesler N, Saritas T, Xu Y, Kassner A, Gummert J, Morshuis M, Amrute J, Veltrop RJA, Boor P, Klingel K, Van Laake LW, Vink A, Hoogenboezem RM, Bindels EMJ, Schurgers L, Sattler S, Schapiro D, Schneider RK, Lavine K, Milting H, Costa IG, Saez-Rodriguez J, Kramann R, Spatial multi-omic map of human myocardial infarction, Nature 608 (2022) 766–777. [PubMed: 35948637]

[22]. Madissoon E, Oliver AJ, Kleshchevnikov V, Wilbrey-Clark A, Polanski K, Orsi AR, Mamanova L, Bolt L, Richoz N, Elmentaite R, Pett JP, Huang N, He P, Dabrowska M, Pritchard S, Tuck L, Prigmore E, Knights A, Oszlanczi A, Hunter A, Vieira SF, Patel M, Georgakopoulos N, Mahbubani K, Saeb-Parsy K, Clatworthy M, Bayraktar OA, Stegle O, Kumasaka N, Teichmann SA, Meyer KB, A spatial multi-omics atlas of the human lung reveals a novel immune cell survival niche, bioRxiv (2021), 2021.2011.2026.470108.

[23]. Moffitt JR, Bambah-Mukku D, Eichhorn SW, Vaughn E, Shekhar K, Perez JD, Rubinstein ND, Hao J, Regev A, Dulac C, Zhuang X, Molecular, spatial, and functional single-cell profiling of the hypothalamic preoptic region, Science 362 (2018).

[24]. Alon S, Goodwin DR, Sinha A, Wassie AT, Chen F, Daugharthy ER, Bando Y, Kajita A, Xue AG, Marrett K, Prior R, Cui Y, Payne AC, Yao CC, Suk HJ, Wang R, Yu CJ, Tillberg P, Reginato P, Pak N, Liu S, Punthambaker S, Iyer EPR, Kohman RE, Miller JA, Lein ES, Lako A, Cullen N, Rodig S, Helvie K, Abravanel DL, Wagle N, Johnson BE, Klughammer J, Slyper M, Waldman J, Jane-Valbuena J, Rozenblatt-Rosen O, Regev A, Consortium I, Church GM, Marblestone AH, Boyden ES, Expansion sequencing: spatially precise in situ transcriptomics in intact biological systems, Science 371 (2021).

[25]. Kebschull JM, Richman EB, Ringach N, Friedmann D, Albarran E, Kolluru SS, Jones RC, Allen WE, Wang Y, Cho SW, Zhou H, Ding JB, Chang HY, Deisseroth K, Quake SR, Luo L, Cerebellar nuclei evolved by repeatedly duplicating a conserved cell-type set, Science 370 (2020).

[26]. Ortiz C, Navarro JF, Jurek A, Martin A, Lundeberg J, Meletis K, Molecular atlas of the adult mouse brain, Sci. Adv. 6 (2020) eabb3446. [PubMed: 32637622]

[27]. Boogerd CJ, Lacraz GPA, Vertesy A, van Kampen SJ, Perini I, de Ruiter H, Versteeg D, Brodehl A, van der Kraak P, Giacca M, de Jonge N, Junker JP, van Oudenaarden A, Vink A, van Rooij E, Spatial transcriptomics unveils ZBTB11 as a regulator of cardiomyocyte degeneration in arrhythmogenic cardiomyopathy, Cardiovasc. Res. 119 (2) (2022) 477–491.

[28]. Osterhout JA, Kapoor V, Eichhorn SW, Vaughn E, Moore JD, Liu D, Lee D, DeNardo LA, Luo L, Zhuang X, Dulac C, A preoptic neuronal population controls fever and appetite during sickness, Nature 606 (2022) 937–944. [PubMed: 35676482]

[29]. Pujadas E, Beaumont M, Shah H, Schrode N, Francoeur N, Shroff S, Bryce C, Grimes Z, Gregory J, Donnelly R, Fowkes ME, Beaumont KG, Sebra R, Cordon-Cardo C, Molecular Profiling of Coronavirus Disease, (COVID-19) autopsies uncovers novel disease mechanisms, Am. J. Pathol. 191 (2021) (2019) 2064–2071.

[30]. Park J, Foox J, Hether T, Danko DC, Warren S, Kim Y, Reeves J, Butler DJ, Mozsary C, Rosiene J, Shaiber A, Afshin EE, MacKay M, Rendeiro AF, Bram Y, Chandar V, Geiger H, Craney A, Velu P, Melnick AM, Hajirasouliha I, Beheshti A, Taylor D, Saravia-Butler A, Singh U, Wurtele ES, Schisler J, Fennessey S, Corvelo A, Zody MC, Germer S, Salvatore S, Levy S, Wu S, Tatonetti NP, Shapira S, Salvatore M, Westblade LF, Cushing M, Rennert H, Kriegel AJ, Elemento O, Imielinski M, Rice CM, Borczuk AC, Meydan C, Schwartz RE, Mason CE, System-wide transcriptome damage and tissue identity loss in COVID-19 patients, Cell Rep. Med. 3 (2022), 100522. [PubMed: 35233546]

[31]. Ma F, Hughes TK, Teles RMB, Andrade PR, de Andrade Silva BJ, Plazyo O, Tsoi LC, Do T, Wadsworth MH 2nd, Oulee A, Ochoa MT, Sarno EN, Iruela-Arispe ML, Klechevsky E, Bryson B, Shalek AK, Bloom BR, Gudjonsson JE, Pellegrini M, Modlin RL, The cellular architecture of the antimicrobial response network in human leprosy granulomas, Nat. Immunol. 22 (2021) 839–850. [PubMed: 34168371]

[32]. Boyd DF, Allen EK, Randolph AG, Guo XJ, Weng Y, Sanders CJ, Bajracharya R, Lee NK, Guy CS, Vogel P, Guan W, Li Y, Liu X, Novak T, Newhams MM, Fabrizio TP, Wohlgemuth N, Mourani PM, Investigators PPICI, Wight TN, Schultz-Cherry S, Cormier SA, Shaw-Saliba K, Pekosz A, Rothman RE, Chen KF, Yang Z, Webby RJ, Zhong N, Crawford JC, Thomas PG, exuberant fibroblast activity compromises lung function via ADAMTS4, Nature 587 (2020) 466–471. [PubMed: 33116313]

[33]. Janosevic D, Myslinski J, McCarthy TW, Zollman A, Syed F, Xuei X, Gao H, Liu YL, Collins KS, Cheng YH, Winfree S, El-Achkar TM, Maier B, Melo Ferreira R, Eadon MT, Hato T, Dagher PC, The orchestrated cellular and molecular responses of the kidney to endotoxin define a precise sepsis timeline, Elife 10 (2021).

[34]. Maniatis S, Aijo T, Vickovic S, Braine C, Kang K, Mollbrink A, Fagegaltier D, Andrusivova Z, Saarenpaa S, Saiz-Castro G, Cuevas M, Watters A, Lundeberg J, Bonneau R, Phatnani H, Spatiotemporal dynamics of molecular pathology in amyotrophic lateral sclerosis, Science 364 (2019) 89–93. [PubMed: 30948552]

[35]. Welch GM, Boix CA, Schmauch E, Davila-Velderrain J, Victor MB, Dileep V, Bozzelli PL, Su Q, Cheng JD, Lee A, Leary NS, Pfenning AR, Kellis M, Tsai LH, Neurons burdened by DNA double-strand breaks incite microglia activation through antiviral-like signaling in neurodegeneration, Sci. Adv. 8 (2022) eabo4662. [PubMed: 36170369]

[36]. Galeano Nino JL, Wu H, LaCourse KD, Kempchinsky AG, Baryiames A, Barber B, Futran N, Houlton J, Sather C, Sicinska E, Taylor A, Minot SS, Johnston CD, Bullman S, Effect of the intratumoral microbiota on spatial and cellular heterogeneity in cancer, Nature 611 (2022) 810–817. [PubMed: 36385528]

[37]. Karras P, Bordeu I, Pozniak J, Nowosad A, Pazzi C, Van Raemdonck N, Landeloos E, Van Herck Y, Pedri D, Bervoets G, Makhzami S, Khoo JH, Pavie B, Lamote J, Marin-Bejar O, Dewaele M, Liang H, Zhang X, Hua Y, Wouters J, Browaeys R, Bergers G, Saeys Y, Bosisio F, van den Oord J, Lambrechts D, Rustgi AK, Bechter O, Blanpain C, Simons BD, Rambow F, Marine JC, A cellular hierarchy in melanoma uncouples growth and metastasis, Nature 610 (2022) 190–198. [PubMed: 36131018]

[38]. Househam J, Heide T, Cresswell GD, Spiteri I, Kimberley C, Zapata L, Lynn C, James C, Mossner M, Fernandez-Mateos J, Vinceti A, Baker AM, Gabbutt C, Berner A, Schmidt M, Chen B, Lakatos E, Gunasri V, Nichol D, Costa H, Mitchinson M, Ramazzotti D, Werner B, Iorio F, Jansen M, Caravagna G, Barnes CP, Shibata D, Bridgewater J, Rodriguez-Justo M, Magnani L, Sottoriva A, Graham TA, Phenotypic plasticity and genetic control in colorectal cancer evolution, Nature 611 (2022) 744–753. [PubMed: 36289336]

[39]. Xu L, Zou C, Zhang S, Chu TSM, Zhang Y, Chen W, Zhao C, Yang L, Xu Z, Dong S, Yu H, Li B, Guan X, Hou Y, Kong FM, Reshaping the systemic tumor immune environment (STIE) and tumor immune microenvironment (TIME) to enhance immunotherapy efficacy in solid tumors, J. Hematol. Oncol. 15 (2022) 87. [PubMed: 35799264]

[40]. Hu B, Sajid M, Lv R, Liu L, Sun C, A review of spatial profiling technologies for characterizing the tumor microenvironment in immuno-oncology, Front. Immunol. 13 (2022), 996721. [PubMed: 36389765]

[41]. Berglund E, Maaskola J, Schultz N, Friedrich S, Marklund M, Bergenstrahle J, Tarish F, Tanoglidi A, Vickovic S, Larsson L, Salmen F, Ogris C, Wallenborg K, Lagergren J, Stahl P, Sonnhammer E, Helleday T, Lundeberg J, Spatial maps of prostate cancer transcriptomes reveal an unexplored landscape of heterogeneity, Nat. Commun. 9 (2018) 2419. [PubMed: 29925878]

[42]. Wu Y, Yang S, Ma J, Chen Z, Song G, Rao D, Cheng Y, Huang S, Liu Y, Jiang S, Liu J, Huang X, Wang X, Qiu S, Xu J, Xi R, Bai F, Zhou J, Fan J, Zhang X, Gao Q, Spatiotemporal immune landscape of colorectal cancer liver metastasis at single-cell level, Cancer Discov. 12 (2022) 134–153. [PubMed: 34417225]

[43]. Guilliams M, Bonnardel J, Haest B, Vanderborght B, Wagner C, Remmerie A, Bujko A, Martens L, Thone T, Browaeys R, De Ponti FF, Vanneste B, Zwicker C, Svedberg FR, Vanhalewyn T, Goncalves A, Lippens S, Devriendt B, Cox E, Ferrero G, Wittamer V, Willaert A, Kaptein SJF, Neyts J, Dallmeier K, Geldhof P, Casaert S, Deplancke B, Ten Dijke P, Hoorens A, Vanlander A, Berrevoet F, Van Nieuwenhove Y, Saeys Y, Saelens W, Van Vlierberghe H, Devisscher L, Scott CL, Spatial proteogenomics reveals distinct and evolutionarily conserved hepatic macrophage niches, Cell 185 (2022) 379–396 e338. [PubMed: 35021063]

[44]. Brbic M, Cao K, Hickey JW, Tan Y, Snyder MP, Nolan GP, Leskovec J, Annotation of spatially resolved single-cell data with STELLAR, Nat. Methods 19 (2022) 1411–1418. [PubMed: 36280720]

[45]. Lu Y, Liu M, Yang J, Weissman SM, Pan X, Katz SG, Wang S, Spatial transcriptome profiling by MERFISH reveals fetal liver hematopoietic stem cell niche architecture, Cell Discov. 7 (2021) 47. [PubMed: 34183665]

[46]. Zhang M, Eichhorn SW, Zingg B, Yao Z, Cotter K, Zeng H, Dong H, Zhuang X, Spatially resolved cell atlas of the mouse primary motor cortex by MERFISH, Nature 598 (2021) 137–143. [PubMed: 34616063]

[47]. Fang R, Xia C, Close JL, Zhang M, He J, Huang Z, Halpern AR, Long B, Miller JA, Lein ES, Zhuang X, Conservation and divergence of cortical cell organization in human and mouse revealed by MERFISH, Science 377 (2022) 56–62. [PubMed: 35771910]

[48]. Kathe C, Skinnider MA, Hutson TH, Regazzi N, Gautier M, Demesmaeker R, Komi S, Ceto S, James ND, Cho N, Baud L, Galan K, Matson KJE, Rowald A, Kim K, Wang R, Minassian K, Prior JO, Asboth L, Barraud Q, Lacour SP, Levine AJ, Wagner F, Bloch J, Squair JW, Courtine G, The neurons that restore walking after paralysis, Nature 611 (2022) 540–547. [PubMed: 36352232]

[49]. Luca BA, Steen CB, Matusiak M, Azizi A, Varma S, Zhu C, Przybyl J, Espin-Perez A, Diehn M, Alizadeh AA, van de Rijn M, Gentles AJ, Newman AM, Atlas of clinically distinct cell states and ecosystems across human solid tumors, Cell 184 (2021), 5482–5496 e5428. [PubMed: 34597583]

[50]. Zhao N, Zhang Y, Cheng R, Zhang D, Li F, Guo Y, Qiu Z, Dong X, Ban X, Sun B, Zhao X, Spatial maps of hepatocellular carcinoma transcriptomes highlight an unexplored landscape of heterogeneity and a novel gene signature for survival, Cancer Cell Int. 22 (2022) 57. [PubMed: 35109839]

[51]. Nagasawa S, Kuze Y, Maeda I, Kojima Y, Motoyoshi A, Onishi T, Iwatani T, Yokoe T, Koike J, Chosokabe M, Kubota M, Seino H, Suzuki A, Seki M, Tsuchihara K, Inoue E, Tsugawa K, Ohta T, Suzuki Y, Genomic profiling reveals heterogeneous populations of ductal carcinoma in situ of the breast, Commun. Biol. 4 (2021) 438. [PubMed: 33795819]

[52]. Zugazagoitia J, Gupta S, Liu Y, Fuhrman K, Gettinger S, Herbst RS, Schalper KA, Rimm DL, Biomarkers associated with beneficial PD-1 checkpoint blockade in non-small cell lung Cancer (NSCLC) identified using high-Plex digital spatial Profiling, Clin. Cancer Res. 26 (2020) 4360–4368. [PubMed: 32253229]

[53]. Gouin KH 3rd, Ing N, Plummer JT, Rosser CJ, Ben Cheikh B, Oh C, Chen SS, Chan KS, Furuya H, Tourtellotte WG, Knott SRV, Theodorescu D, An N-cadherin 2 expressing epithelial cell subpopulation predicts response to surgery, chemotherapy and immunotherapy in bladder cancer, Nat. Commun. 12 (2021) 4906. [PubMed: 34385456]

[54]. Jung SH, Hwang BH, Shin S, Park EH, Park SH, Kim CW, Kim E, Choo E, Choi IJ, Swirski FK, Chang K, Chung YJ, Spatiotemporal dynamics of macrophage heterogeneity and a potential function of Trem2(hi) macrophages in infarcted hearts, Nat. Commun. 13 (2022) 4580. [PubMed: 35933399]

[55]. Downes Damien J, Cross Amy R, Hua Peng, Roberts Nigel, Schwessinger Ron, Cutler Antony J, Munis Altar M, Brown Jill, Mielczarek Olga, Carlos E de Andrea, Melero Ignacio; COvid-19 Multi-omics Blood ATlas (COMBAT) Consortium; Gill Deborah R, Hyde Stephen C, Knight Julian C, Todd John A, Sansom Stephen N, Issa Fadi, Davies James O J, Hughes Jim R, Identification of LZTFL1 as a candidate effector gene at a COVID-19 risk locus, Nat. Genet. 53 (2021) 1606–1615. [PubMed: 34737427]

[56]. Petitprez F, de Reynies A, Keung EZ, Chen TW, Sun CM, Calderaro J, Jeng YM, Hsiao LP, Lacroix L, Bougouin A, Moreira M, Lacroix G, Natario I, Adam J, Lucchesi C, Laizet YH, Toulmonde M, Burgess MA, Bolejack V, Reinke D, Wani KM, Wang WL, Lazar AJ, Roland CL, Wargo JA, Italiano A, Sautes-Fridman C, Tawbi HA, Fridman WH, B cells are associated with survival and immunotherapy response in sarcoma, Nature 577 (2020) 556–560. [PubMed: 31942077]

[57]. Italiano A, Bessede A, Pulido M, Bompas E, Piperno-Neumann S, Chevreau C, Penel N, Bertucci F, Toulmonde M, Bellera C, Guegan JP, Rey C, Sautes-Fridman C, Bougouin A, Cantarel C, Kind M, Spalato M, Dadone-Montaudie B, Le Loarer F, Blay JY, Fridman WH, Pembrolizumab in soft-tissue sarcomas with tertiary lymphoid structures: a phase 2 PEMBROSARC trial cohort, Nat. Med. 28 (2022) 1199–1206. [PubMed: 35618839]

[58]. Mavropoulos A, Johnson C, Lu V, Nieto J, Schneider EC, Saini K, Phelan ML, Hsie LX, Wang MJ, Cruz J, Mei J, Kim JJ, Lian Z, Li N, Boutet SC, Wong-Thai AY, Yu W, Lu QY, Kim T, Geng Y, Masaeli MM, Lee TD, Rao J, Artificial intelligence-driven morphology-based enrichment of malignant cells from body fluid, Mod. Pathol. 36 (2023), 100195. [PubMed: 37100228]

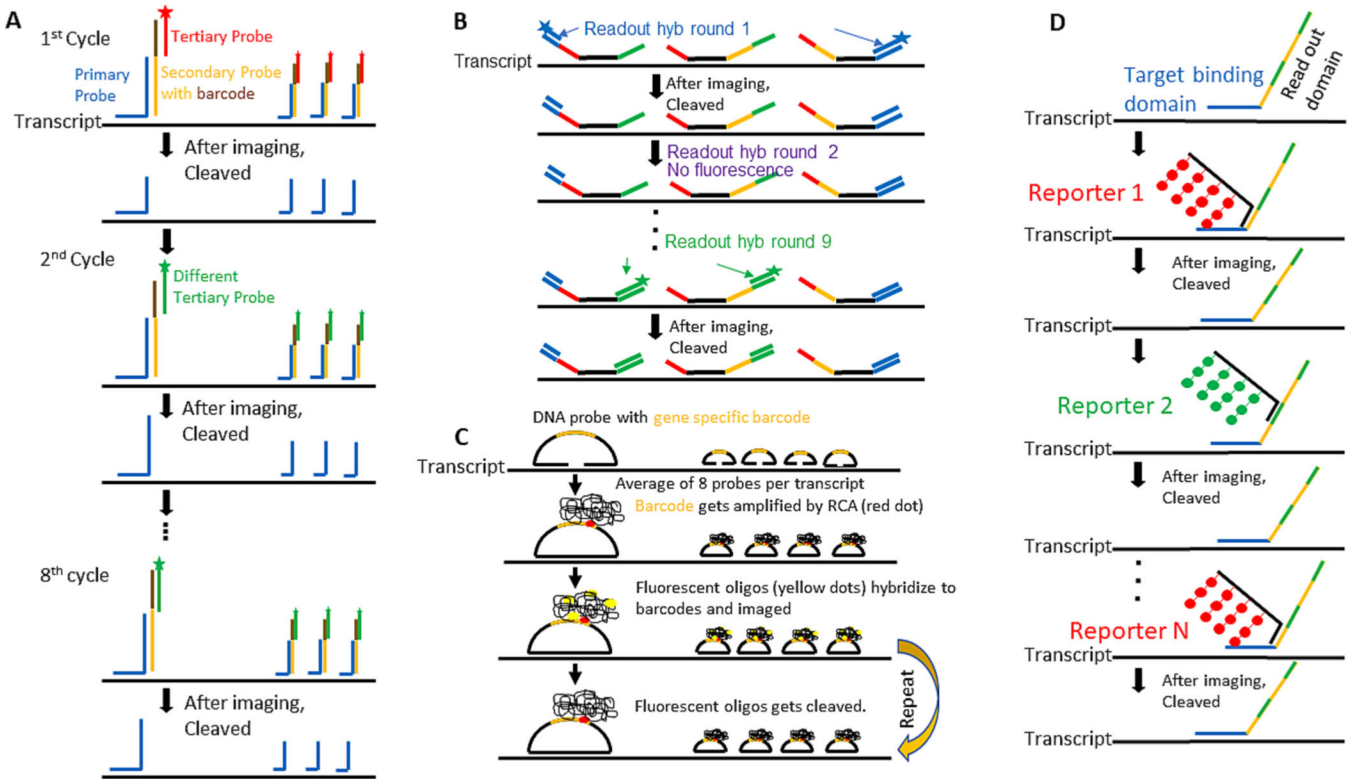

Fig. 1.

Schematic depiction of different probe hybridization and imaging strategies of 4 imaging-based spatial transcriptomics technologies. A) Molecular Cartography technology-a three-probe hybridization strategy. B) MERSCOPE-a two-probe hybridization strategy. The secondary probes are only fluorescently labeled in some of the hybridization rounds. C) Xenium-a Padlock probe-based hybridization strategy. Gene-specifc ligation increases in hybridization specificity. D) CosMx SMI-a modified two-probe hybridization strategy. The primary probe has 16 read-out domain and the secondary probe contains multiple dyes to increase signal intensity.

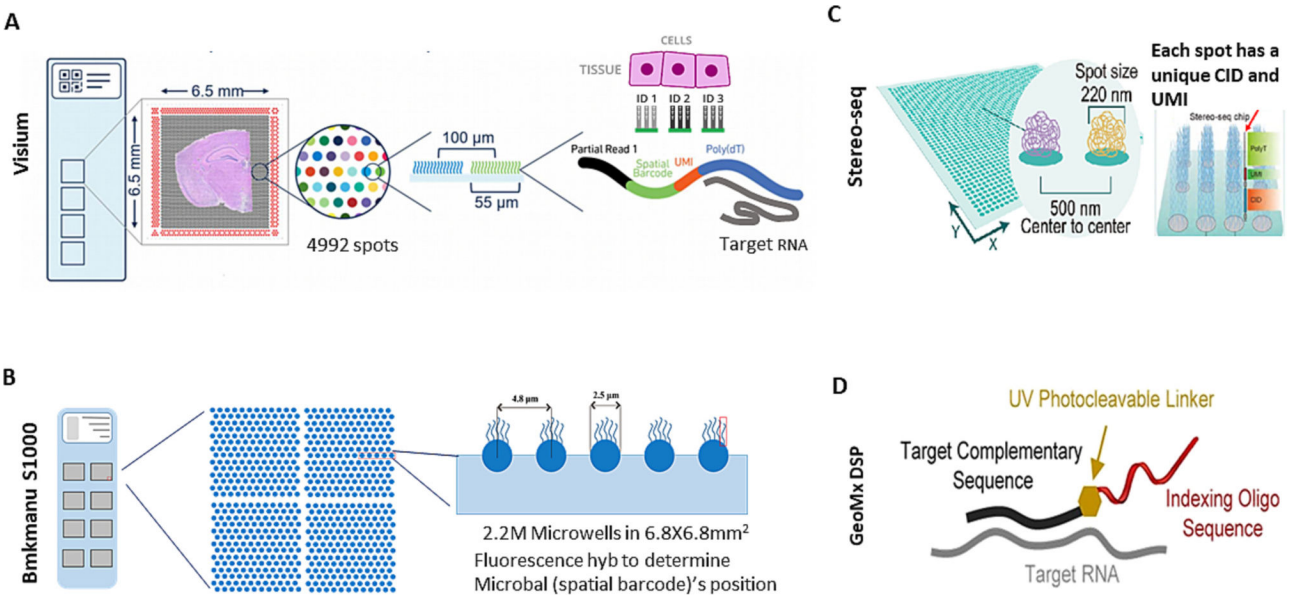

Fig. 2.

Core technologies of 4 sequencing-based platforms. Visium (A), S1000 (B) and Stereo-sEq. (C) use probes mounted on the array to capture RNA for library construction and sequencing. The key difference among those 3 platforms is spot size (A > B > C), which determines spatial resolution. GeoMx DSP (D) uses a probe hybridization strategy. Each probe is linked with a gene-specifc barcode through a UV cleavable linker. The barcodes are cleaved from the selected region of interest, and collected for library construction and sequencing. UMI: Unique Molecule Identifier. CID: Coordinate Identity. The pink box located in the upper right corner of B indicates a probe comprising Read1 handle, a spatial barcode, UMI, and PolyT.

Table 1

Key parameters of 8 spatial transcriptome platforms.

	Platform	# of genes profiled	Spatial Resolution	RNA Capture efficiency	Tmaging Area	Time Required
Imaging-Based	Molecular Cartography	100	275 nm	>90%	Total ROTs ≤ = 26 mm^2	3.5–4 days
	MERSCOPE	500	100 nm	95% for cells 80–85% for tissue	10 mm × 10 mm	28–30 h
	Xenium	400	50 nm	Not Available	12 mm × 24 mm	2 days
	CosMX SMI	1000	50 nm	Not Available	20mmX15mm	3 days-1 week
Sequencing-Based	10 × Visium	Whole Transcriptome	100um	Not Available	(6.5 mm × 6.5 mm)X4	<1 h
	GeoMx DSP	Whole Transcriptome	50um	Not Available	35.3 mm × 14.1 mm	<1 h
	BMKMANU S1000	Whole Transcriptome	4.8um	4962/100um^2	(6.8 mm × 6.8 mm)X8	<1 h
	Stereo-Seq	Whole Transcriptome	0.5um	12,661/100um^2	10 mm × 10 mm 13.2 cm × 13.2 cm	<1 h